Published in final edited form as:

J Immunol. 2010 April 1; 184(7): 3743–3754. doi:10.4049/jimmunol.0903164.

Loss of T Cell and B Cell Quiescence Precedes the Onset of Microbial Flora-Dependent Wasting Disease and Intestinal Inflammation in Gimap5-Deficient Mice

Michael J. Barnes[*,1], **Halil Aksoylar**[†,1], **Philippe Krebs**[*], **Tristan Bourdeau**[†], **Carrie N. Arnold**[*], **Yu Xia**[*], **Kevin Khovananth**[*], **Isaac Engel**[‡], **Sosathya Sovath**[*], **Kristin Lampe**[†], **Eleana Laws**[†], **Amy Saunders**[§], **Geoffrey W. Butcher**[§], **Mitchell Kronenberg**[‡], **Kris Steinbrecher**[†], **David Hildeman**[†], **H. Leighton Grimes**[†], **Bruce Beutler**[*], and **Kasper Hoebe**[†]

[*]Department of Genetics, Scripps Research Institute, La Jolla

[†]Cincinnati Children's Hospital Research Foundation, Cincinnati, OH 45229

[‡]La Jolla Institute for Allergy and Immunology, San Diego, CA 92037

[§]The Babraham Institute, Babraham Research Campus, Cambridge, United Kingdom

Abstract

Homeostatic control of the immune system involves mechanisms that ensure the self-tolerance, survival and quiescence of hematopoietic-derived cells. In this study, we demonstrate that the GTPase of immunity associated protein (Gimap)5 regulates these processes in lymphocytes and hematopoietic progenitor cells. As a consequence of a recessive *N*-ethyl-*N*-nitrosourea–induced germline mutation in the P-loop of Gimap5, lymphopenia, hepatic extramedullary hematopoiesis, weight loss, and intestinal inflammation occur in homozygous mutant mice. Irradiated fetal liver chimeric mice reconstituted with Gimap5-deficient cells lose weight and become lymphopenic, demonstrating a hematopoietic cell-intrinsic function for Gimap5. Although Gimap5-deficient $CD4^+$ T cells and B cells appear to undergo normal development, they fail to proliferate upon Ag-receptor stimulation although NF-κB, MAP kinase and Akt activation occur normally. In addition, in Gimap5-deficient mice, $CD4^+$ T cells adopt a $CD44^{high}$ $CD62L^{low}$ $CD69^{low}$ phenotype and show reduced IL-7rα expression, and T-dependent and T-independent B cell responses are abrogated. Thus, Gimap5-deficiency affects a noncanonical signaling pathway required for Ag-receptor–induced proliferation and lymphocyte quiescence. Antibiotic-treatment or the adoptive transfer of Rag-sufficient splenocytes ameliorates intestinal inflammation and weight loss, suggesting that immune responses triggered by microbial flora causes the morbidity in Gimap5-deficient mice. These data establish Gimap5 as a key regulator of hematopoietic integrity and lymphocyte homeostasis.

Address correspondence and reprint requests to Kasper Hoebe, Cincinnati Children's Hospital Research Foundation, MLC7021, Room S5.421, 3333 Burnet Avenue, Cincinnati, OH 45229. kasper.hoebe@cchmc.org.

[1]M.J.B. and H.A. contributed equally to this article.

The online version of this article contains supplemental material.

Disclosures

The authors have no financial conflicts of interest.

Many layers of regulation ensure homeostatic control of the immune system during development and throughout life. In fetal and neonatal mice, hematopoietic stem cells (HSCs) and precursor cells migrate from the fetal liver to the bone marrow and thymus (1). Thereafter, maintenance of the HSC niche involves both cell-extrinsic and cell-intrinsic mechanisms in which responsiveness to growth factors, cell cycle control, and breakdown of metabolic by-products are essential (2). When these processes occur normally, the many diverse lineages of hematopoietic cells are continually generated in the bone marrow and thymus. Given their potential to undergo clonal expansion and long-term survival, additional checkpoints are needed to limit the survival of self-reactive T cells and B cells (3). In T cells, these checkpoints include the induction of apoptosis in thymocytes that recognize self-Ags with high affinity (negative selection) (4) and the mitigation of inappropriate immune responses by regulatory T cells (5). The availability of common–γ-chain cytokines governs the size and composition of the T cell niche (6–8). Notably, IL-2, IL-7, and IL-15 promote T cell survival by modulating the expression of Bcl-2–family member proteins.

Somewhat paradoxically, mutations or conditions that partially impair T cell survival can be associated with the development of immunopathologies (9). One potential explanation for this association is that excess common–γ-chain cytokines available in lymphopenic conditions allow the survival and proliferation of self-reactive T cell clones. For example, when naive $CD4^+$ T cells are transferred into Rag-deficient recipient mice, they undergo lymphopenia-induced proliferation (LIP) and adopt a characteristic phenotype similar to memory $CD4^+$ T cells that includes the expression of increased amounts of CD44 ($CD44^{high}$) and reduced amounts of CD62L ($CD62L^{low}$), whereas CD69 expression remains mostly unaffected ($CD69^{low}$) (8, 10). In some genetic backgrounds, intestinal microbial florae promote the expansion of colitogenic IFN-γ–producing $CD4^+$ T cells undergoing LIP, resulting in intestinal inflammation (11). Congenitally lymphopenic *Tcrα*$^{-/-}$ mice also develop intestinal inflammation owing to excessive IL-4–dependent Th2 cell and γδ T cell responses (12–14). Lymphopenia has also been linked to the precipitation of diabetes in animal models (15, 16). Increased rates of T cell turnover, altered ratios of regulatory to conventional T cells, and acquisition of effector function by T cells undergoing LIP are all aspects of the lymphopenic environment that might favor the onset of immunopathology.

Homozygosity for the *lyp* mutation causes severe T cell lymphopenia and has been shown to predispose rats to the development of autoimmune diabetes (16) and intestinal inflammation (17). However, lymphopenia caused by the *lyp* mutation alone is insufficient to trigger immunopathology, which requires the presence of additional modifier alleles at other loci in the genome (17–21). In both susceptible and disease-free genetic backgrounds, homozygous *lyp* rats largely lack $CD8^+$ T cells and have reduced $CD4^+$ T cell and NKR-$P1^+$ NKT cell numbers (21–23), whereas deficiencies in conventional B cells have not been reported (24). Positional cloning efforts identified the *lyp* mutation as a frameshift mutation in the gene *Gimap5* (also known as *Ian4*, *Ian5*, or *Irod*) (25).

The *Gimap* genes (previously known as immune-associated nucleotide binding proteins [*Ian*]) comprise a family of genes that are physically clustered in the genome and predominantly expressed in lymphocytes (26). The cellular localization and functions of the GTP ase of immunity-associated proteins (Gimap) remain nebulous. All Gimap proteins

share a GTP-binding AIG1 homology domain, which was originally identified in a gene involved in plant immunity (27). In mammals, evidence suggests that Gimap3 and Gimap5 both promote thymocyte and T cell survival (26, 28–30), whereas Gimap4 can limit T cell viability (31, 32). More recently, *Gimap5*$^{-/-}$ mice were reported to have decreased numbers of peripheral T cells, similar to the *lyp* rat, and also showed disrupted development of NK cells, reduced survival of Vα14 TCR-expressing invariant NKT (*iNKT*) cells, granulocyte accumulation, increased hepatocyte apoptosis and early mortality (33). Thus, the effect of complete Gimap5-deficiency in mice is much more severe than the truncation of Gimap5 by the *lyp* mutation in rats.

These discrepancies open several new avenues for investigation into the function of Gimap5 in vivo. First, although liver failure caused by hepatocyte apoptosis in *Gimap5*$^{-/-}$ mice was suggested (33), the cause of the early morbidity in these mice remained unclear. In addition, despite the report of decreased B1 cell accumulation in the peritoneum of *Gimap5*$^{-/-}$ mice (33), the effect of Gimap5-deficiency on B cell development was not examined, nor was the role of Gimap5 in thymocyte selection or peripheral T cell and B cell function explored. In this study, we describe a recessive *N*-ethyl-*N*-nitrosourea (ENU)–induced mutation in *Gimap5*, which we termed sphinx. Like *Gimap5*$^{-/-}$ mice, *sphinx* homozygotes are lymphopenic, show granulocyte accumulation, exhibit liver abnormalities, and die by 14 weeks old. Using the *sphinx* mouse, we demonstrate that *Gimap5* serves previously uncharacterized cell-intrinsic roles in lymphocyte survival, quiescence, and Ag-receptor induced proliferation, and link the early morbidity in *sphinx* mice to suppressible, microbial flora-dependent, intestinal inflammation and wasting disease.

Materials and Methods

Mice and reagents

All experiments were performed according to the U.S. National Institutes of Health guidelines and were approved by the Institutional Animal Care and Use Committee of The Scripps Research Institute (TSRI) and The Cincinnati Children's Hospital. *BALB/cJ*, *Bim*$^{-/-}$, *C57BL/6J*, *Cd4*$^{-/-}$, *Cd8*$^{-/-}$, *DBA/ 2J*, *FVB/NJ*, and *NODShiLtJ* mice were obtained from The Jackson Laboratory (Bar Harbor, ME). β*2m*$^{-/-}$, *C3H/HeN*, *H-Y TCR* transgenic, *Rag2*$^{-/-}$, and *Rag2*$^{-/-}$ *Il2rγ*$^{-/-}$ mice were obtained from Taconic (Germantown, NY). *Gimap5*$^{sph/sph}$ mice were generated at TSRI using ENU mutagenesis. Jα18$^{-/-}$ mice were housed at the La Jolla Institute for Allergy and Immunology and *act-mOVA* transgenic mice were housed at TSRI. All mice were maintained under specific pathogen-free conditions.

αGal-Cer–mouse CD1d tetramers labeled with PE or APC were generated as described previously (34), and all Abs used for flow cytometry were purchased from eBioscience(SanDiego, CA) or BioLegend (SanDiego, CA). Abs for immunoblotting were purchased from Cell Signaling Technology (Beverly, MA). Purified CD3ε (145-2C11) and CD28 (37.51) abs (eBioscience) were used for T cell activation. F(ab′)$_2$–anti-IgM (Jackson ImmunoResearch), anti-CD40 (eBioscience), rIL-4 (R&D Systems, Minneapolis, MN), LPS (Axxora, San Diego, CA) and PMA/ionomycin (Sigma-Aldrich, St. Louis, MO) were used for B cell activation. T cells and B cells were labeled with CFSE by incubating MACS (Miltenyi Biotech, Auburn, CA) purified CD4$^+$ T cells or splenic B cells in 5 μMCFSE in

PBS with 0.1% FCS for 10 min. ELISAs were used to measure serum cytokine concentrations (eBioscience).

In vivo cytotoxicity assay measuring NK cell and CD8$^+$ T cell function

We immunized G3 ENU mice with 1×10^7 γ-irradiated (1500 rad) act-mOVA splenocytes. Seven days later, we injected 1×10^7 CFSE-labeled cells i.v., consisting of a mixture of three different splenocyte populations (C57BL/6J, β*2m*$^{-/-}$, and SIINFEKL-peptide pulsed C57BL/6J splenocytes) at a ratio of 1:1:1. After 48 h, blood was drawn from the retro-orbital plexus, RBCs were lysed, and the presence or absence of each CFSE-labeled cell population was determined by flow cytometry.

mAb MAC421 against mouse Gimap5

A glutathione-S-transferase fusion protein containing residues 1–270 of mouse Gimap5 was produced using *Escherichia coli* RosettaDE3 bacteria (Novagen, Madison, WI). Purification was performed by elution from glutathione beads and used to immunize a LEW rat. The rat was euthanized 3 d after a final boost with this immunogen, isolated splenocytes were fused with the plasmacytoma cell line Y3Ag1.2.3 (35), and hybridomas were derived by standard methods. The selected clone MAC421 secretes a rat IgG2a Ab specific for Gimap5—that is, it shows no cross-reactivity on other members of the mouse Gimap family. Separate studies have shown that the epitope recognized by MAC421 is dependent on residues 1–10 at the NH2 terminus of mouse Gimap5 (C. Carter, G.W. Butcher, T. Nitta, K. Yano, and Y. Takahama, unpublished observations).

Complete blood counts

Blood samples were taken from the retro-orbital plexus of mice at indicated ages and analyzed using a Hemavet 950 veterinary hematology system Fisher Scientific (Pittsburgh, PA).

Hepatic lymphoid cell isolation

Mice were euthanized using CO_2, and livers were flushed with ice cold PBS via the hepatic portal vein using a 25-gauge needle and syringe. After excision of the liver, the gall bladder was removed and livers were diced using scissors. Further homogenization was achieved using a sieve and plunger, and liver fragments were gently passed through a 100-μM strainer and collected in a 50-ml centrifuge tube. Total liver cells were washed with 40 ml ice-cold RPMI 1640/5% FBS and centrifuged for 10 min at 300 × g. The resulting pellets were resuspended in digestion medium (RPMI 1640 containing 0.02% [w/v] collagenase IV [Sigma-Aldrich] and 0.002% [w/v] DNase I [Sigma-Aldrich]) and left at 37°C for 40 min under gentle shaking. Ice cold serum free medium was added to each tube, and cells were centrifuged for 3 min at 30 × g and 4°C. Supernatants containing lymphocyte-enriched cell populations were collected and centrifuged at 300 × g for 10 min and 4°C. Subsequently, cell pellets were resuspended in PBS containing 0.5% FBS and labeled with the mouse Lineage Cell Depletion Kit (Miltenyi Biotec). Lin$^-$ cells were then separated using an AutoMacs magnetic sorter (Miltenyi Biotec), and various HSCs or precursor populations were identified by flow cytometry as described before (36).

Ab responses

For T-dependent Ab responses, age- and sex-matched mice were immunized i.p. with 5 μg LPS (Axxora) and 50 μg of NP36-CGG (Biosearch Technologies, Novato, CA) mixed 1:1 with alum (Pierce, Rockford, IL). For T-independent Ab responses, mice were immunized i.p. with 50 μg NP50-Ficoll (Biosearch Technologies). Serum NP-specific Abs were detected by ELISA. Briefly, 96-well round-bottom plates (Fisher Scientific) were coated with 5 μg/ml NP30-BSA (Biosearch Technologies) for detection of NP-specific Ig. Serum samples from immunized mice were serially diluted in 1% milk and added to coated or uncoated (to determine background) wells. Plates were incubated with HRP-conjugated goat anti-mouse IgM or IgG1 (Southern Biotechnology Associates, Birmingham, AL), developed with Peroxidase Substrate and Stop Solution (KPL), and measured for absorbance at 450 nm.

Immunoblotting

Immunoblotting was performed using total spleen, thymus, or bone marrow lysates, or splenic B cells that were isolated using MACS purification with anti-CD19 microbeads (Miltenyi Biotech). Cell lysis and immunoblotting were performed as described previously (37).

Cell cycle analysis of splenic B cells

Splenic B cells were cultured with complete IMDM (containing 10% FCS and 1% P/S) and left untreated or treated with 0.1 μg/ml LPS at 37°C, 5% CO_2. After 48 h, 1×10^6 cells were collected in 1 ml PBS and subsequently were added dropwise to 2.5 ml absolute ethyl alcohol. After 15 min fixation on ice, cells were washed with PBS and incubated in 500 μl propidium iodide (PI) solution (50 μg/ml PI, 0.1 mg/ml RNase A, and 0.05% Triton X-100 in PBS) for 40 min at 37°C. Cells were washed and resuspended in PBS and subsequently analyzed by flow cytometry.

Antibiotic treatment and survival assays

Gimap5$^{+/sph}$ breeding pairs received antibiotic treatment (1 g/l ampicillin, 500 mg/l vancomycin, 1 g/l neomycin sulfate, and 1 g/l metronidazole) administered orally via drinking water. Subsequent litters remained on antibiotic treatment until analysis at 9-wk-old. For adoptive transfer studies, *Gimap5*$^{sph/sph}$ mice at 25235 d old were injected i.v. with 1×10^7 splenocytes that had been depleted of RBCs (RBC lysis buffer; Sigma-Aldrich). Mice were monitored and euthanized according to veterinarian recommendations when they became moribund.

Statistical analysis

Data were analyzed using the GraphPad Prism4 software (GraphPad Software, San Diego, CA). Unless indicated otherwise, statistical significance of the differences among groups was determined from the mean and SD by Student's two-tailed test or by ANOVA followed by Dunnett's test for three or more groups. All data were considered statistically significant if $p < 0.05$.

Results

sphinx: an ENU-induced germline mutation causing severe lymphopenia

We identified *sphinx* in a forward genetic screen designed to detect defective in vivo cytotoxic NK cell and $CD8^+$ T cell responses in G3-ENU mutagenized mice (38). The original *sphinx* founder, previously immunized with OVA-expressing cells, was unable to reject adoptively transferred NK cell or $CD8^+$ T cell target cells (Fig. 1*A*). Necropsy revealed a near absence of $CD8^+$ T cells and NK cells in the peripheral lymphoid organs (Fig. 1*B*, 1*C*) and a marked reduction in total T cell numbers. However, relatively normal thymocyte development occurred, including the $CD4^+$ T cell, $CD8^+$ T cell, γδ T cell, $Foxp3^+$ regulatory T cell, and *i*NKT cell lineages (data not shown), whereas the bone marrow contained a high frequency of NK cells expressing the activation marker CD69 (Supplemental Fig. 1). Most strikingly, *sphinx* livers exhibited an abnormal morphology that presented itself as extramedullary hematopoiesis with associated foci of hematopoietic cells (Fig. 1*D*, 1*E*). Hyperplastic nodules developed in adult livers (Fig. 1*D*) that contained well-differentiated hepatocytes bordered by clusters of hematopoietic cells (Fig. 1*E*). Hepatocytes from *sphinx* mice showed no growth advantage in cell culture and no dysplastic liver cells were observed throughout this study (M. Barnes and K. Hoebe, unpublished observations). In addition, when *sphinx* mice (C57BL/ 6J genetic background) were crossed with mice of one of five different genetic backgrounds (BALB/cJ, C3H/HeN, DBA/2J, FVB/ NJ, or NOD/ShiLtJ) for two generations and then intercrossed, the liver phenotype remained consistent and dysplastic cells were not observed in any other organs (data not shown). Thus,it appeared that *sphinx* livers exhibited an abnormal morphology owing to extramedullary hematopoiesis and reactive hyperplasia of hepatocytes, rather than a hepatic neoplasia. In addition, *sphinx* mice progressively developed normocytic anemia (Fig. 1*F*, Supplemental Fig. 2*A*), with increased variation in RBC width (Supplemental Fig. 2*B*) and thrombocytopenia (Supplemental Fig. 2*C*). This was correlated with a rapid reduction in circulating blood lymphocytes (Fig. 1*G*) and concomitant neutrophilia (Supplemental Fig. 2*D*). These observations indicated that the *sphinx* mutation affected a gene essential for lymphocyte maintenance and normal hematopoiesis.

Positional cloning of the *sphinx* mutation

To identify the causative mutation, we used a positional cloning strategy (39). Using 13 meioses from *sphinx* mice backcrossed to the C3H/HeN strain, we linked the NK cell and $CD8^+$ T cell deficiency to chromosome 6 with a peak LOD score of 4.0 (Supplemental Fig. 3*A*). Further fine mapping with 572 meioses derived from F1 intercrosses confined the mutation to a 2.9-megabase critical region, bounded by the microsatellite markers D6mit315 and D6mit276. We amplified and sequenced all annotated and predicted coding base pairs in the critical region, obtaining high-quality sequence for 89.9% of total coding base pairs and 100% of coding base pairs for genes in the *Gimap* cluster. Among 1.74×10^5 bp sequenced, a single G→T point mutation in the *Gimap5* coding region differed between the *sphinx* and C57BL/6J genomes (Supplemental Fig. 3*B*, 3*C*). *Gimap5* is predominantly transcribed in lymphocytes (26), but is also expressed in HSCs (40). The *sphinx* mutation appeared to destabilize the Gimap5 protein in hematopoietic tissues, including total bone marrow cells

and splenic B cells, resulting in a lack of detectable protein (Fig. 1*H*), whereas mRNA expression of *Gimap5* remained unaffected (Fig. 1*I*).

The *sphinx* mutation resulted in the amino acid substitution G38C, which changed an amino acid that is highly conserved within all mouse *Gimap* homologs and within all annotated orthologous genes containing an AIG1 domain, in kingdoms as distant as Planta and Protista (Supplemental Fig. 3*D*). This residue is located in the predicted P-loop of the AIG1 domain of Gimap5, in the pocket that binds and hydrolyzes GTP. Previous studies of the p21Ras GTPase have shown that mutation of the analogous Gly residue to Val (G15V) resulted in a protein that was unable to hydrolyze GTP or to transform NIH 3T3 cells when overexpressed (41). The mutation of this residue to Cys might destabilize Gimap5 by altering the disulphide bonding patterns of the mutant Gimap5 protein. Whereas no Gimap5 protein was detected by immunoblotting, any residual intact protein below the limit of detection would be predicted to be nonfunctional because of the mutation of the conserved Gly residue. Overall, the *sphinx* phenotype mirrors the phenotype of previously described *Gimap5*$^{-/-}$ mice (33), indicating that the *sphinx* mutation effectively results in a Gimap5-null animal.

Lethal wasting disease, colitis, and hepatic extramedullary hematopoiesis in *sphinx* mice

From birth until weaning, conventionally housed *sphinx* (hereafter *Gimap5*$^{sph/sph}$) mice appeared outwardly healthy. After 4 wk, males showed a reduced growth rate (Fig. 2*A*) and developed diarrhea. Although significant, weight loss in females was less dramatic and only occurred after 6 wk (data not shown). In male and female *Gimap5*$^{sph/sph}$ mice, cell infiltration and inflammation were observed in the colon by 6 wk. Severe colitis, exemplified by goblet cell depletion, leukocyte infiltration into the lamina propria, epithelial cell hyperplasia, and crypt loss, developed by 10 wk (Fig. 2*B*). Wasting disease and intestinal inflammation likely contributed to the early morbidity of *Gimap5*$^{sph/sph}$ mice, which generally occurred by 14 wk.

Liver dysfunction remained another possible factor contributing to early morbidity. To better understand the onset of liver abnormalities, we investigated the development of the embryonic and neonatal liver. At the embryonic day (ED) 16 developmental stage and at birth, livers from *Gimap5*$^{sph/sph}$ mice and their heterozygous littermates appeared similar (Fig. 2*C*). However, more hematopoietic cells remained in *Gimap5*$^{sph/sph}$ livers at day 8. By day 14, extramedullary hematopoiesis could be observed before the initiation of nodule formation. Extramedullary hematopoiesis, which persisted in adult mice, was limited to the liver (Fig. 3*A*), although a disrupted splenic architecture that included reduced follicle size and number and granulocyte accumulation was also observed (data not shown). Schulteis et al. (33) argued that *Gimap5*$^{-/-}$ mice die as a consequence of liver dysfunction and hepatocyte apoptosis. Despite the abnormal liver morphology, we found normal concentrations of serum bilirubin and albumin in 8-wk-old *Gimap5*$^{sph/sph}$ mice (data not shown), suggesting that the metabolic functions of the liver remained largely intact.

Cell-intrinsic hematopoietic defects in Gimap5$^{sph/sph}$ mice

We next considered that aberrant hematopoiesis rather than liver failure might contribute to wasting disease and mortality in *Gimap5*$^{sph/sph}$ mice. Despite the liver abnormalities, the bone marrow of 5-wk-old *Gimap5*$^{sph/sph}$ mice contained normal numbers of Lin$^-$ Sca1$^+$ c-Kit$^+$ HSCs and hematopoietic progenitor cells (Supplemental Fig. 4 *A*, *B*). However, the numbers of megakaryocyte/erythroid progenitors (MEPs) declined with age, in correlation with the onset of anemia and thrombocytopenia in adult *Gimap5*$^{sph/sph}$ mice (Fig. 1*F*, Supplemental Fig. 2*C*). In addition, despite normal numbers of common lymphoid progenitors (CLPs) in the bone marrow, rapid atrophy of the thymus occurred with age (data not shown). More dramatic differences were observed in the *Gimap5*$^{sph/sph}$ liver. Examination of hematopoietic progenitor cell populations revealed that a significant number of HSCs and hematopoietic precursors, representing all hematopoietic lineages, remained in the adult *Gimap5*$^{sph/sph}$ liver (Fig. 3*A*). Compared to normal hematopoiesis in the bone marrow, extramedullary liver hematopoiesis in *Gimap5*$^{sph/sph}$ mice was skewed toward generation of Lin$^-$ Sca1$^+$ c-Kit$^-$ IL-7rα$^+$ CLPs, and it is noteworthy that IL-7rα expression was increased in this population (Fig. 3*A*).

To investigate the functionality of *Gimap5*$^{sph/sph}$ HSCs, we made radiation bone marrow and fetal liver chimeras. Similar to what was reported for *Gimap5*$^{-/-}$ mice (33), *Gimap5*$^{sph/sph}$ bone marrow cells poorly reconstituted the hematopoietic compartment of lethally irradiated congenic recipient mice (data not shown), suggesting functional impairment. To exclude the possibility that defective HSC function was a secondary consequence of the inflammation and wasting disease that occurs in *Gimap5*$^{sph/sph}$ mice, we reconstituted lethally irradiated *Rag2*$^{-/-}$ *Il2r*γ$^{-/-}$ recipients with *Gimap5*$^{sph/sph}$ or *Gimap5*$^{sph/+}$ littermate control ED 19 fetal liver cells. The recipients were chosen because they lacked endogenous T cells, B cells, and NK cells, but could support the development of a normal lymphocyte compartment from wild type HSCs. Six weeks after transfer, mice reconstituted with *Gimap5*$^{sph/sph}$ fetal liver cells were severely lymphopenic and had substantially fewer thymocytes than mice reconstituted with *Gimap5*$^{sph/+}$ fetal liver cells. In the spleen, CD8$^+$ T cell, B cell, and NK cell numbers were markedly reduced compared with recipients of control fetal liver cells, whereas CD4$^+$ T cells were present at normal numbers (Fig. 3*B*). *Gimap5*$^{sph/sph}$ fetal liver cell recipients exhibited weight loss and wasting, whereas control fetal liver cell recipients appeared healthy (data not shown). In *Gimap5*$^{sph/sph}$ fetal liver cell recipients, CD11b$^+$ Gr1$^+$ myeloid cells accumulated in the spleen (Fig. 3*B*), whereas liver abnormalities were not observed. The transfer of weight loss and wasting disease, but not liver abnormalities, by *Gimap5*$^{sph/sph}$ fetal liver cells suggested that the early mortality observed in *Gimap5*$^{sph/sph}$ mice is at least partially caused by defective hematopoiesis. Furthermore, the *Gimap5*$^{sph/sph}$ fetal liver cells exhibited an intrinsic defect in lymphopoiesis, affecting T cells, B cells, and NK cells.

Reduced survival and IL-7rα expression in Gimap5$^{sph/sph}$ T cells

Several mouse models have linked impaired lymphocyte function and lymphopenia with the development of various manifestations of immunopathology (9, 15). To better understand the contribution of lymphocytes to the hematopoietically transferrable abnormalities observed in *Gimap5*$^{sph/sph}$ mice, we investigated lymphocyte development, survival and

function. Roles for Gimap5 in T cells have been proposed for thymic selection, thymic export, and survival in the periphery (16). Like *Gimap5*$^{lyp/lyp}$ rats and *Gimap5*$^{-/-}$ mice, 6-wk-old *Gimap5*$^{sph/sph}$ mice exhibited normal thymus cellularity and frequencies of DN1–4, DP, CD4 SP, and CD8 SP thymocyte subpopulations (data not shown). To examine thymic selection in *Gimap5*$^{sph/sph}$ thymocytes, we bred the mutation onto the H-Y TCR transgenic background. The H-Y TCR recognizes an endogenous peptide presented by MHC class I molecules that is derived from the H-Y Ag, which is expressed only in male mice. Consequently, H-Y TCR$^+$ thymocytes are normally deleted by negative selection in male mice, whereas they develop into mature CD8$^+$ T cells in female mice. In *Gimap5*$^{sph/sph}$ males, H-Y–reactive thymocytes were deleted, implying that the mutation did not impede negative selection (Fig. 4*A*). In contrast, the thymus of *Gimap5*$^{sph/sph}$ females contained normal numbers of H-Y TCR$^+$ DP thymocytes, but significantly fewer H-Y TCR$^+$ CD8 SP thymocytes (Fig. 4*A*), suggesting that positively selected thymocytes became more sensitive to proapoptotic negative selection cues in the absence of Gimap5. H-Y TCR$^+$ CD8$^+$ T cells were found at reduced numbers and frequencies in the spleen of both male and female *Gimap5*$^{sph/sph}$ mice (Fig. 4*B*), indicating that lymphopenia occurred regardless of TCR specificity for self-Ag.

We next examined the expression of molecules important for thymic egress and peripheral accumulation of T cells. Normally, terminally differentiated TCRβ$^+$ CD4 SP and CD8 SP thymocytes upregulate CD5 and IL-7rα (CD127) and downregulate CD24 (HSA) and CD69 (4, 42). *Gimap5*$^{sph/sph}$ CD8 SP, but not CD4 SP thymocytes, failed to modulate CD24, CD69, or IL-7rα expression (Fig. 4*C*), suggesting that the mutation either blocked terminal CD8 SP thymocyte maturation or impaired survival of CD8 SP cells. Downregulation of CD69 expression has been associated with the ability of thymocytes to exit the thymus (43), and it is possible that export of CD8 SP thymocytes is impaired in *Gimap5*$^{sph/sph}$ mice. In addition, as IL-7 promotes naive T cell survival by modulating expression of anti-apoptotic molecules (44), reduced IL-7rα expression in *Gimap5*$^{sph/sph}$ CD8 SP thymocytes likely contributes to the failure of CD8$^+$ T cells to survive and accumulate in the periphery.

CD4$^+$ T cells isolated from the spleen of 6-wk-old *Gimap5*$^{sph/sph}$ mice showed a significant reduction in IL-7rα surface expression (Fig. 4*D*) and were unable to proliferate upon TCR stimulation (Fig. 4*E*). Thus, impaired IL-7 signaling and TCR-induced proliferation represent two contributing factors to the CD4$^+$ T cell lymphopenia in *Gimap5*$^{sph/sph}$ mice. As the lymphopenia became more pronounced with age (Fig. 1*G*), CD4$^+$ T cells began to express cell-surface markers characteristic of cells undergoing LIP, including reduced amounts of CD62L but normal, low expression of CD69 (Fig. 4*F*).

We also noted that peripheral *Gimap5*$^{sph/sph}$ *i*NKT cells expressed reduced amounts of NK1.1 (Fig. 5*A*) and rapidly declined in number with age. NK1.1 expression is acquired at a late step in *i*NKT cell differentiation, most typically after export from the thymus, and evidence suggests that it requires engagement of the invariant TCR with the CD1d Ag-presenting molecule (45). Upon in vivo activation of *i*NKT cells with the agonist αGal-Cer, we detected little intracellular IFN-γ or TNF-α, reduced amounts of IL-4 and normal amounts of IL-13 on a per cell basis (Fig. 5*B*). We confirmed these results by ELISA (Fig. 5*C*). The impaired survival of *i*NKT cells and aberrant *i*NKT cell cytokine response that

occurs in *Gimap5*$^{sph/sph}$ mice suggests roles for Gimap5 in both lymphocyte survival and function.

Functional defects in Gimap5$^{sph/sph}$ B cells

Before the onset of wasting disease, splenic CD19^{+} B cells in *Gimap5*$^{sph/sph}$ mice, unlike T cells and NK cells, were less reduced in number compared with C57BL/6J littermates. However, the B cell compartment contained fewer mature B cells (Fig. 6*A*), whereas the percentages of marginal zone B cells (Fig. 6*B*) and follicular B cells (Fig. 6*C*) were similar to C57BL/6J littermates. Between 6–10 wk, splenic B cell numbers declined in *Gimap5*$^{sph/sph}$ mice (Supplemental Fig. 5*A*). In the peritoneal cavity, few B1 cells were found (M. Barnes and K. Hoebe, unpublished data), suggesting that B1 cells either fail to develop or survive. In addition, the serum of 8-wk-old *Gimap5*$^{sph/sph}$ mice contained ~75% less IgM and 50% less total IgG than heterozygous littermates (Supplemental Fig. 5*B*). The reduced total IgG reflected significant reductions in concentrations of the isotypes IgG1, IgG2b, and IgG3 and a trend toward reduced Ig-G2a (Supplemental Fig. 5*B*). These abnormalities suggested the possibility that B cell function was impaired in *Gimap5*$^{sph/sph}$ mice. To assess B cell function, we immunized 6-wk-old mice with T-dependent (NP-CGG + alum + LPS) or T-independent (NP-ficoll) Ags. *Gimap5*$^{sph/sph}$ mice failed to produce either T-dependent Ag-specific IgG1 Abs (Fig. 6*D*) or T-independent Ag-specific IgM responses (Fig. 6*E*), suggesting that *Gimap5*$^{sph/sph}$ B cells might have an intrinsic functional defect. To investigate B cell-intrinsic signaling, we isolated B cells from 6-wk-old *Gimap5*$^{sph/sph}$ and C57BL/6J mice and determined their capacity to proliferate upon activation in vitro. *Gimap5*$^{sph/sph}$ B cells failed to proliferate after BCR stimulation, or treatment with the diacylglycerol mimetic, PMA, and the Ca^{++} mobilizing agent ionomycin (Fig. 6*F*). However, alternative pathways triggered by LPS or CD40 ligation induced normal *Gimap5*$^{sph/sph}$ B cell proliferation (Fig. 6*F*).

Activation of the NF-κB, MAP kinase, and Akt pathways is essential for either BCR or PMA and ionomycin induced proliferation. We examined the activation of these pathways in *Gimap5*$^{sph/sph}$ B cells stimulated with PMA and ionomycin. Normal degradation of the NF-κB inhibitor IκB and phosphorylation of the Erk, Jnk, and p38 MAP kinases occurred (Supplemental Fig. 5*C*). In addition, normal activation of Akt, marked by phosphorylation of serine and threonine residues, and other proximal molecules in the Akt pathway was observed (Supplemental Fig. 5*D*). Nonetheless, *Gimap5*$^{sph/sph}$ B cells failed to proliferate upon PMA and ionomycin activation. Ex vivo cell cycle analysis of *Gimap5*$^{sph/sph}$ B cells detected an increased percentage of B cells in S phase and a reduced number of B cells in G2 phase. When proliferation was induced with LPS, an equivalent number of *Gimap5*$^{sph/sph}$ B cells entered G2 phase, yet an increased percentage of cells remained in S phase (Fig. 6*G*), suggesting that defective cycling might cause the decline in peripheral B cell numbers in *Gimap5*$^{sph/sph}$ mice (Supplemental Fig. 5*A*). Overall, we found no major defects in proximal mitogenic signaling or cell cycle entry, but we did find aberrant cell cycle progression in *Gimap5*$^{sph/sph}$ B cells.

Prevention of wasting disease and intestinal inflammation, but not lymphopenia, by antibiotic treatment

Microbial flora in the intestine represents the major reservoir of foreign Ags and exogenous innate immune stimuli in specific pathogen-free housed mice. Localized inflammation in the gastrointestinal tract of *Gimap5*$^{sph/sph}$ mice suggested the possibility that aberrant responses triggered by microbial flora contributed to systemic CD4$^+$ T cell LIP and subsequent cell death, ultimately resulting in lymphopenia. Thus, we sought to address the role of microbial flora in *Gimap5*$^{sph/sph}$ mice. Homozygotes and hetero-zygote littermates were put on a continuous antibiotic regimen from birth until 9 wk, when they were analyzed. Interestingly, antibiotic treatment did not prevent lymphopenia (Fig. 7*A*), the expression of CD44^{high} CD62L^{low} markers by CD4$^+$ T cells (Fig. 7*B*) or the occurrence of hepatic extramedullary hematopoiesis and hepatocyte hyperplasia (Fig. 7*C*). Antibiotic-treatment completely blocked the accumulation of CD11b$^+$ myeloid cells (Fig. 7*A*), ameliorated intestinal inflammation (Fig. 7*C*), and prevented weight loss (data not shown) in *Gimap5*$^{sph/sph}$ mice. These data suggest that the Gimap5-dependent hematopoietic cell-intrinsic phenotypes, including hepatic extramedullary hematopoiesis, lymphopenia, and acquisition of a CD44^{high} CD62L^{low} phenotype by CD4$^+$ T cells, can occur in the absence of intestinal inflammation, whereas microbial florae promote granulocyte accumulation, colitis, and wasting disease.

Adoptively transferred lymphocytes reduce extramedullary hematopoiesis and early mortality in Gimap5$^{sph/sph}$ mice

To further assess the involvement of lymphocytes in the immunopathology observed in *Gimap5*$^{sph/sph}$ mice, we adoptively transferred 1×10^7 congenically labeled C57BL/6J splenocytes into young *Gimap5*$^{sph/sph}$ mice before the onset of wasting disease. Strikingly, recipient *Gimap5*$^{sph/sph}$ mice did not succumb to early death (Fig. 8*A*) or develop wasting disease (Fig. 8*B*). Adoptively transferred splenocytes filled the CD8$^+$ T cell niche (Fig. 8*C*) and promoted the maintenance of endogenous *Gimap5*$^{sph/sph}$ CD4$^+$ T cells (Fig. 8*D*). In the CD4$^+$ T cell compartment, cells of *Gimap5*$^{sph/sph}$ origin retained a CD44^{high} CD62L^{low} phenotype (Fig. 8*E*). Thus, adoptively transferred splenocytes promoted the accumulation of endogenous *Gimap5*$^{sph/sph}$ CD4$^+$ T cells, but not CD8$^+$ T cells.

We also examined whether adoptively transferred C57BL/6J splenocytes affected the extramedullary hematopoiesis in recipient *Gimap5*$^{sph/sph}$ mice. In the liver of untreated 15-wk-old *Gimap5*$^{sph/sph}$ mice, an abundance of common myeloid progenitors were present, including both granulocyte/macrophage progenitors (GMPs) and MEPs. In the livers of age-matched *Gimap5*$^{sph/sph}$ mice that received adoptively transferred C57BL/6J splenocytes, clusters of hematopoietic cells, nodules, and extramedullary hematopoiesis were still observed, but at a reduced frequency (Supplemental Fig. 6*A*, 6*B*) and fewer common myeloid progenitor, MEP, and CLP cells were found (Fig. 8*F*, Supplemental Fig. 6*B*). In addition, the bone marrow of aged *Gimap5*$^{sph/sph}$ mice showed enhanced granulopoiesis and reduced erythropoiesis (Fig. 8*G*). These changes in medullary hematopoiesis likely contributed to the neutrophilia (Supplemental Fig. 2*D*) and anemia (Fig. 1*G*) observed in adult *Gimap5*$^{sph/sph}$ mice. Recipients of adoptively transferred splenocytes maintained normal numbers and frequencies of GMP and MEP in the bone marrow (Fig. 8*G*), indicating

that transferred cells also affected medullary hematopoiesis. Accordingly, recipient *Gimap5*$^{sph/sph}$ mice did not become anemic or exhibit thymic atrophy (data not shown). Enhanced granulopoiesis and thymic atrophy are often observed in conditions of chronic inflammation, and their amelioration by either antibiotics or the adoptive transfer of splenocytes suggests that they are most likely triggered by the inflammatory environment present in *Gimap5*$^{sph/sph}$ mice.

Finally, we observed no reduction in mortality or wasting disease when *Gimap5*$^{sph/sph}$ mice received *Rag2*$^{-/-}$ splenocytes, indicating that a lymphocyte population is required to prevent wasting disease (Fig. 8*A*). Because adoptively transferred *Cd4*$^{-/-}$, *Cd8*$^{-/-}$, or *Jα18*$^{-/-}$ (*iNKT* cell-deficient) splenocytes, or anti-NK1.1 Ab depleted splenocytes could each prevent weight loss and early mortality (data not shown), multiple lymphocyte populations might contribute to the suppression of wasting disease.

Discussion

Our identification and subsequent characterization of the *sphinx* mutation confirms the nonredundant role of *Gimap5* in lymphocyte survival and normal hematopoiesis (33). The *Gimap5*$^{sph/sph}$ mouse exhibits a number of hematologic abnormalities. From birth, peripheral CD8^{+} T cells and NK cells fail to accumulate, whereas HSCs accumulate in the liver, suggesting that Gimap5 has a direct role in controlling these processes. After weaning, intestinal inflammation, weight loss, severe lymphopenia, and acquisition of a CD44^{high} CD62L^{low} CD69^{low} phenotype characteristic of cells undergoing LIP by CD4^{+} T cells all occur before premature death at ~14-wk-old. We used several approaches to examine the relationships between these phenotypes. Fetal liver HSCs, which were not exposed to the inflammatory environment present in adult *Gimap5*$^{sph/sph}$ mice, could transfer wasting disease and lymphopenia to lethally irradiated recipients, demonstrating an HSC intrinsic function for *Gimap5*. Wasting disease and colitis were mitigated by adoptively transferred lymphocytes, indicating that either defective immune regulation or a lymphopenic environment, or both, contributed to the onset of intestinal inflammation. Antibiotic-sensitive microbes were also required to trigger granulocyte accumulation, wasting disease and intestinal inflammation, but not lymphopenia or accumulation of CD44^{high} CD62L^{low} CD69^{low} CD4^{+} T cells.

Before the onset of post weaning abnormalities, extramedullary hematopoiesis occurred in the *Gimap5*$^{sph/sph}$ neonatal liver. Defective HSC egress or migration from the neonatal liver could underlie this phenomenon. One possibility that we favor is that *Gimap5*$^{sph/sph}$ HSCs become activated in the neonatal liver, thereby halting their migration and inducing extramedullary hematopoiesis. For example, HSC express Toll-like receptors and can undergo myelopoiesis at extramedullary sites in response to LPS-induced inflammation (46, 47). Gimap5 might act as a negative regulator of HSC activation, initiated by TLR agonists or other stimuli, that maintains quiescence of the HSC niche. In young *Gimap5*$^{sph/sph}$ mice, these abnormalities appear to be limited to the liver, and hematopoietic abnormalities in the bone marrow were observed only in older mice, concurrent with granulocyte accumulation and chronic inflammation. Further studies will be needed to determine whether *Gimap5*$^{sph/sph}$ bone marrow HSCs have reduced reconstituting capacity because of the

chronically inflamed *Gimap5*$^{sph/sph}$ environment or because of a cell-intrinsic requirement for Gimap5 that becomes more pronounced with age.

In addition to aberrant hematopoiesis, intestinal inflammation contributed to the weight loss and early morbidity in *Gimap5*$^{sph/sph}$ mice. Spontaneous mouse models of colitis have proven valuable in identifying molecules and mechanisms involved in the pathogenesis of inflammatory bowel disease (48). An abundance of IL-13–producing NKT cells are found in the intestinal lamina propria of human ulcerative colitis patients (49), and IL-13–producing *i*NKT cells can drive colitis in a mouse model induced by the chemical oxazolone (50). Our data suggest that the *Gimap5*$^{sph/sph}$ environment favors the polarization of *i*NKT cells toward the production of IL-13. Although the cellular and molecular basis of intestinal inflammation in *Gimap5*$^{sph/sph}$ mice demands further dissection, IL-13–producing *i*NKT cells may represent one contributing factor. Another potential influence predisposing *Gimap5*$^{sph/sph}$ mice to developing colitis is CD4$^+$ T cells undergoing LIP. In the naive CD4$^+$ T cell transfer model of colitis, using C57BL/6 Rag-deficient recipient strains, the lymphopenic environment drives CD4$^+$ T cells in to LIP. These CD4$^+$ T cells undergoing LIP acquire effector function and cause both intestinal inflammation and wasting disease (11). Of note, intestinal inflammation is significantly reduced when naive T cells are transferred into germ-free mice, suggesting that microbial florae are necessary for colitogenic immune responses in this model (51). The presence of microbial flora might similarly promote the acquisition of effector function among intestinal CD4$^+$ T cells undergoing LIP in *Gimap5*$^{sph/sph}$ mice. Interestingly, in partially lymphopenic settings such as in sublethally γ-irradiated mice, colitis is not observed after naive T cell transfer (8). Residual radioresistant intestinal lymphocytes that enhance intestinal barrier function, such as IgA-secreting plasma cells or γδ T cells, might limit colitogenic CD4$^+$ T cell responses in this setting (8, 52).In *Gimap5*$^{sph/sph}$ mice, the loss of non-CD4$^+$ lymphocytes with age might generate conditions that promote CD4$^+$ T cells to undergo LIP, and thereby contribute to the onset of intestinal inflammation.

Our findings that *Gimap5*$^{sph/sph}$ HSCs were unable to reconstitute the B cell compartment of irradiated recipients, and that *Gimap5*$^{sph/sph}$ B cells were unable to undergo Ag-receptor induced proliferation or generate Ag-specific IgG or IgM responses were especially surprising. In the *lyp* rat model, *lyp* bone marrow cells are able to normally reconstitute the B cell compartment of irradiated recipients (30) and gross B cell functional defects are not observed (24). This discrepancy might reflect different requirements for Gimap proteins in rats and mice. The *Gimap* gene cluster has undergone divergent evolution between rodent species, including changes in the number of *Gimap* genes, amino acid sequence variation between homologous Gimap proteins, and differential Gimap gene expression patterns in lymphocytes (26, 53). To characterize better the consequences of Gimap5-deficiency in mouse B cells, we first considered that Gimap5 might be involved in the activation of the NF-κB and MAP kinase signaling pathways by BCR stimulation, because others had reported that these pathways are dysregulated in *lyp* T cells (54). However, *Gimap5*$^{sph/sph}$ mice have normal percentages of marginal zone B cells, which require NF-κB signaling to develop (55), and display normal IκB degradation and MAP kinase phosphorylation upon activation. Normal activation of the PI3K/Akt pathway, which is similarly required for

lymphocyte proliferation, also occurs in *Gimap5*$^{sph/sph}$ B cells. One interesting attribute of *Gimap5*$^{sph/sph}$ B cells is their accumulation in S phase in vivo. The role for Gimap5 in cell cycle regulation appears to be especially important in the bone marrow or fetal liver cell reconstitution setting, in which donor cells must undergo rapid proliferation to reconstitute the B cell niche. In summary, Gimap5 impairs BCR-induced proliferation and Ig responses independently of activation of the canonical BCR signaling pathways and may link BCR triggering to cell cycle progression.

Although the requirement for Gimap5 in TCR-dependent T cell proliferation and survival has been known for some time, our study identifies several important mechanisms that fail to operate in *Gimap5*$^{sph/sph}$ T cells. In the thymus, developing *Gimap5*$^{sph/sph}$ CD8 SP thymocytes show impaired survival after positive selection and reduced expression of IL-7rα, suggesting that Gimap5 modulates survival thresholds during thymic selection as well as the expression of a critical cytokine receptor for T cell survival. Although CD4 SP thymocytes express normal amounts of IL-7rα, expression is reduced in the periphery among CD4$^+$ T cells. These findings provide a partial molecular basis for previous observations made in the lyp rat (16) and *Gimap5*$^{-/-}$ mouse (33). In these strains, and in *Gimap5*$^{sph/sph}$ mice, CD8$^+$ T cells and naive CD4$^+$ T cells, which are more dependent on IL-7 for their survival than Ag-experienced or regulatory CD4$^+$ T cells (56), are most affected by Gimap5-deficiency. As discussed below, IL-7–independent mechanisms regulating T cell survival also appear to require Gimap5. The net effect of Gimap5 deficiency in CD4$^+$ T cells is to promote the accumulation of cells with a CD44^{high} CD62L^{low} LIP-like phenotype with the potential to cause immunopathology. Importantly, other factors such as MHC haplotype and modifier alleles are needed to cause diabetes (18–20) and, as we have shown in this study, microbial florae are required for the onset of colitis. Finally, although peripheral CD4$^+$ Foxp3$^+$ regulatory T cell numbers are minimally affected in *Gimap5*$^{sph/sph}$ mice, it is not known whether they function and express a normal TCR repertoire, or whether the lymphopenic environment inhibits their ability to control aberrant immune responses. Alternatively, a Foxp3$^-$ regulatory lymphocyte population might be absent or defective in *Gimap5*$^{sph/sph}$ mice.

Our data identify a critical role for Gimap5 in T cell, B cell, NK cell, *i*NKT cell and HSC survival and function. A previous study reported that Gimap5 might mediate its effects in part by interacting directly with Bcl-2 and a related anti-apoptotic protein Bcl-x_L (26). IL-7rα signaling promotes expression of Bcl-2, which can directly inhibit the proapoptotic activity of Bim (7), and indeed genetic loss of *Bim* restores the T cell compartment in IL-7r–deficient mice (57). Therefore, we considered that *Gimap5*$^{sph/sph}$ *Bim*$^{-/-}$ mice might exhibit less lymphopenia if reduced IL-7rα expression alone prevented T cell accumulation. However, combined Gimap5 and Bim deficiency did not prevent lymphopenia (H. Aksoylar and K. Hoebe, unpublished observations), suggesting that additional survival pathways are perturbed in the absence of Gimap5. Gimap5 may be more than just a prosurvival protein, as it appears to also maintain quiescence in lymphoid cells and HSCs. In support of this possibility, we have found that negative selection thresholds are reduced in thymocytes, HSCs become aberrantly activated in the neonatal liver, and bone marrow NK cells show an activated phenotype. Among B cells, Gimap5 deficiency might in some ways mimic B cell

anergy, which can be induced by constant low-affinity BCR stimulation (58), and might favor the accumulation of B cells in cell cycle arrest. Thus, *Gimap5*$^{sph/sph}$ B cells can proliferate in response to LPS or CD40 stimulation, but, like anergic B cells, fail to respond to BCR stimulation alone. In vivo, activation by weak stimuli that are normally ignored could abrogate quiescence, promoting the accumulation of lymphocytes in cell cycle arrest and driving HSCs to undergo extramedullary hematopoiesis. Future studies will explore the role of pathways important for setting activation thresholds and enforcing quiescence in *Gimap5*$^{sph/sph}$ mice.

Supplementary Material

Refer to Web version on PubMed Central for supplementary material.

Acknowledgments

We thank Dr. Jorge Bezerra and Dr. Ted Denson for insightful discussions, Dr. Mark Jenkins for providing act-mOVA transgenic mice, Amanda Hutchings and Nicholas Pugh for help in generating the MAC421 Ab, and Dr. Argyrios Theofilopoulos and Dr. Rosana Gonzalez-Quintial for discussions and help with the determination of serum Ig isotype concentrations.

This work was supported by National Institutes of Health/National Cancer Institute Grant 1R21CA133649-01, Public Health Service Grant P30 DK078392, NIH 5P01 AI070167, and R37 AI71922, and Competitive Strategic Grant and Ph.D. studentship funding from the U.K. Biotechnology and Biological Sciences Research Council (to G.W.B. and A.S.).

Abbreviations used in this paper

CLP	common lymphoid progenitor
ED	embryonic day
ENU	*N*-ethyl-*N*-nitrosourea
Gimap	GTPase of immunity associated protein
GMP	granulocyte/macrophage progenitor
HSC	hematopoietic stem cell
***i*NKT**	invariant NKT
LIP	lymphopenia-induced proliferation
MEP	megakaryocyteery-throid progenitor
PI	propidium iodide
TSRI	The Scripps Research Institute

References

1. Dzierzak E, Speck NA. Of lineage and legacy: the development of mammalian hematopoietic stem cells. Nat. Immunol. 2008; 9:129–136. [PubMed: 18204427]
2. Tothova Z, Gilliland DG. FoxO transcription factors and stem cell homeostasis: insights from the hematopoietic system. Cell Stem Cell. 2007; 1:140–152. [PubMed: 18371346]

3. Goodnow CC. Multistep pathogenesis of autoimmune disease. Cell. 2007; 130:25–35. [PubMed: 17632054]

4. Palmer E. Negative selection—clearing out the bad apples from the T-cell repertoire. Nat. Rev. Immunol. 2003; 3:383–391. [PubMed: 12766760]

5. Feuerer M, Hill JA, Mathis D, Benoist C. Foxp3+ regulatory T cells: differentiation, specification, subphenotypes. Nat. Immunol. 2009; 10:689–695. [PubMed: 19536194]

6. Ma A, Koka R, Burkett P. Diverse functions of IL-2, IL-15, and IL-7 in lymphoid homeostasis. Annu. Rev. Immunol. 2006; 24:657–679. [PubMed: 16551262]

7. Marrack P, Kappler J. Control of T cell viability. Annu. Rev. Immunol. 2004; 22:765–787. [PubMed: 15032596]

8. Surh CD, Sprent J. Homeostasis of naive and memory T cells. Immunity. 2008; 29:848–862. [PubMed: 19100699]

9. Liston A, Enders A, Siggs OM. Unravelling the association of partial T-cell immunodeficiency and immune dysregulation. Nat. Rev. Immunol. 2008; 8:545–558. [PubMed: 18551129]

10. Murali-Krishna K, Ahmed R. Cutting edge: naive T cells masquerading as memory cells. J. Immunol. 2000; 165:1733–1737. [PubMed: 10925249]

11. Coombes JL, Robinson NJ, Maloy KJ, Uhlig HH, Powrie F. Regulatory T cells and intestinal homeostasis. Immunol. Rev. 2005; 204:184–194. [PubMed: 15790359]

12. Iijima H, Takahashi I, Kishi D, Kim JK, Kawano S, Hori M, Kiyono H. Alteration of interleukin 4 production results in the inhibition of T helper type 2 cell-dominated inflammatory bowel disease in T cell receptor alpha chain-deficient mice. J. Exp. Med. 1999; 190:607–615. [PubMed: 10477546]

13. Mombaerts P, Mizoguchi E, Grusby MJ, Glimcher LH, Bhan AK, Tonegawa S. Spontaneous development of inflammatory bowel disease in T cell receptor mutant mice. Cell. 1993; 75:274–282. [PubMed: 8104709]

14. Nanno M, Kanari Y, Naito T, Inoue N, Hisamatsu T, Chinen H, Sugimoto K, Shimomura Y, Yamagishi H, Shiohara T, et al. Exacerbating role of gammadelta T cells in chronic colitis of T-cell receptor alpha mutant mice. Gastroenterology. 2008; 134:481–490. [PubMed: 18242214]

15. King C, Ilic A, Koelsch K, Sarvetnick N. Homeostatic expansion of T cells during immune insufficiency generates autoimmunity. Cell. 2004; 117:265–277. [PubMed: 15084263]

16. Ramanathan S, Poussier P. BB rat lyp mutation and Type 1 diabetes. Immunol. Rev. 2001; 184:161–171. [PubMed: 12086310]

17. Cousins L, Graham M, Tooze R, Carter C, Miller JR, Powrie FM, Macpherson GG, Butcher GW. Eosinophilic bowel disease controlled by the BB rat-derived lymphopenia/Gimap5 gene. Gastroenterology. 2006; 131:1475–1485. [PubMed: 17064701]

18. Wallis RH, Wang K, Marandi L, Hsieh E, Ning T, Chao GY, Sarmiento J, Paterson AD, Poussier P. Type 1 diabetes in the BB rat: a polygenic disease. Diabetes. 2009; 58:1007–1017. [PubMed: 19168599]

19. Jackson RA, Buse JB, Rifai R, Pelletier D, Milford EL, Carpenter CB, Eisenbarth GS, Williams RM. Two genes required for diabetes in BB rats. Evidence from cyclical intercrosses and backcrosses. J. Exp. Med. 1984; 159:1629–1636. [PubMed: 6202817]

20. Jacob HJ, Pettersson A, Wilson D, Mao Y, Lernmark A, Lander ES. Genetic dissection of autoimmune type I diabetes in the BB rat. Nat. Genet. 1992; 2:56–60. [PubMed: 1303251]

21. Moralejo DH, Park HA, Speros SJ, MacMurray AJ, Kwitek AE, Jacob HJ, Lander ES, Lernmark A. Genetic dissection of lymphopenia from autoimmunity by introgression of mutated Ian5 gene onto the F344 rat. J. Autoimmun. 2003; 21:315–324. [PubMed: 14624755]

22. Elder ME, Maclaren NK. Identification of profound peripheral T lymphocyte immunodeficiencies in the spontaneously diabetic BB rat. J. Immunol. 1983; 130:1723–1731. [PubMed: 6220066]

23. Iwakoshi NN, Greiner DL, Rossini AA, Mordes JP. Diabetes prone BB rats are severely deficient in natural killer T cells. Autoimmunity. 1999; 31:1–14. [PubMed: 10593564]

24. Tullin S, Farris P, Petersen JS, Hornum L, Jackerott M, Markholst H. A pronounced thymic B cell deficiency in the spontaneously diabetic BB rat. J. Immunol. 1997; 158:5554–5559. [PubMed: 9164980]

25. MacMurray AJ, Moralejo DH, Kwitek AE, Rutledge EA, Van Yserloo B, Gohlke P, Speros SJ, Snyder B, Schaefer J, Bieg S, et al. Lymphopenia in the BB rat model of type 1 diabetes is due to a mutation in a novel immune-associated nucleotide (Ian)-related gene. Genome Res. 2002; 12:1029–1039. [PubMed: 12097339]
26. Nitta T, Nasreen M, Seike T, Goji A, Ohigashi I, Miyazaki T, Ohta T, Kanno M, Takahama Y. IAN family critically regulates survival and development of T lymphocytes. PLoS Biol. 2006; 4:e103. [PubMed: 16509771]
27. Poirier GM, Anderson G, Huvar A, Wagaman PC, Shuttleworth J, Jenkinson E, Jackson MR, Peterson PA, Erlander MG. Immune-associated nucleotide-1 (IAN-1) is a thymic selection marker and defines a novel gene family conserved in plants. J. Immunol. 1999; 163:4960–4969. [PubMed: 10528200]
28. Hernández-Hoyos G, Joseph S, Miller NG, Butcher GW. The lymphopenia mutation of the BB rat causes inappropriate apoptosis of mature thymocytes. Eur. J. Immunol. 1999; 29:1832–1841. [PubMed: 10382745]
29. Pandarpurkar M, Wilson-Fritch L, Corvera S, Markholst H, Hornum L, Greiner DL, Mordes JP, Rossini AA, Bortell R. Ian4 is required for mitochondrial integrity and T cell survival. Proc. Natl. Acad. Sci. U.S.A. 2003; 100:10382–10387. [PubMed: 12930893]
30. Ramanathan S, Norwich K, Poussier P. Antigen activation rescues recent thymic emigrants from programmed cell death in the BB rat. J. Immunol. 1998; 160:5757–5764. [PubMed: 9637485]
31. Carter C, Dion C, Schnell S, Coadwell WJ, Graham M, Hepburn L, Morgan G, Hutchings A, Pascall JC, Jacobs H, et al. A natural hypomorphic variant of the apoptosis regulator Gimap4/IAN1. J. Immunol. 2007; 179:1784–1795. [PubMed: 17641045]
32. Schnell S, Démollière C, van den Berk P, Jacobs H. Gimap4 accelerates T-cell death. Blood. 2006; 108:591–599. [PubMed: 16569770]
33. Schulteis RD, Chu H, Dai X, Chen Y, Edwards B, Haribhai D, Williams CB, Malarkannan S, Hessner MJ, Glisic-Milosavljevic S, et al. Impaired survival of peripheral T cells, disrupted NK/NKT cell development, and liver failure in mice lacking Gimap5. Blood. 2008; 112:4905–4914. [PubMed: 18796632]
34. Matsuda JL, Naidenko OV, Gapin L, Nakayama T, Taniguchi M, Wang CR, Koezuka Y, Kronenberg M. Tracking the response of natural killer T cells to a glycolipid antigen using CD1d tetramers. J. Exp. Med. 2000; 192:741–754. [PubMed: 10974039]
35. Galfrè G, Milstein C, Wright B. Rat x rat hybrid myelomas and a monoclonal anti-Fd portion of mouse IgG. Nature. 1979; 277:131–133. [PubMed: 310519]
36. Zarebski A, Velu CS, Baktula AM, Bourdeau T, Horman SR, Basu S, Bertolone SJ, Horwitz M, Hildeman DA, Trent JO, Grimes HL. Mutations in growth factor independent-1 associated with human neutropenia block murine granulopoiesis through colony stimulating factor-1. Immunity. 2008; 28:370–380. [PubMed: 18328744]
37. Kim SO, Jing Q, Hoebe K, Beutler B, Duesbery NS, Han J. Sensitizing anthrax lethal toxin-resistant macrophages to lethal toxin-induced killing by tumor necrosis factor-alpha. J. Biol. Chem. 2003; 278:7413–7421. [PubMed: 12488448]
38. Barnes MJ, Krebs P, Harris N, Eidenschenk C, Gonzalez-Quintial R, Arnold CN, Crozat K, Sovath S, Moresco EM, Theofilopoulos AN, et al. Commitment to the regulatory T cell lineage requires CARMA1 in the thymus but not in the periphery. PLoS Biol. 2009; 7:e51. [PubMed: 19260764]
39. Beutler B, Du X, Xia Y. Precis on forward genetics in mice. Nat. Immunol. 2007; 8:659–664. [PubMed: 17579639]
40. Ng SY, Yoshida T, Zhang J, Georgopoulos K. Genome-wide lineage-specific transcriptional networks underscore Ikaros-dependent lymphoid priming in hematopoietic stem cells. Immunity. 2009; 30:493–507. [PubMed: 19345118]
41. Clanton DJ, Lu YY, Blair DG, Shih TY. Structural significance of the GTP-binding domain of ras p21 studied by site-directed mutagenesis. Mol. Cell. Biol. 1987; 7:3092–3097. [PubMed: 3118192]
42. Egawa T, Tillman RE, Naoe Y, Taniuchi I, Littman DR. The role of the Runx transcription factors in thymocyte differentiation and in homeostasis of naive T cells. J. Exp. Med. 2007; 204:1945–1957. [PubMed: 17646406]

43. Nakayama T, Kasprowicz DJ, Yamashita M, Schubert LA, Gillard G, Kimura M, Didierlaurent A, Koseki H, Ziegler SF. The generation of mature, single-positive thymocytes in vivo is dysregulated by CD69 blockade or overexpression. J. Immunol. 2002; 168:87–94. [PubMed: 11751950]
44. Akashi K, Kondo M, von Freeden-Jeffry U, Murray R, Weissman IL. Bcl-2 rescues T lymphopoiesis in interleukin-7 receptor-deficient mice. Cell. 1997; 89:1033–1041. [PubMed: 9215626]
45. McNab FW, Berzins SP, Pellicci DG, Kyparissoudis K, Field K, Smyth MJ, Godfrey DI. The influence of CD1d in postselection NKT cell maturation and homeostasis. J. Immunol. 2005; 175:3762–3768. [PubMed: 16148122]
46. Massberg S, Schaerli P, Knezevic-Maramica I, Köllnberger M, Tubo N, Moseman EA, Huff IV, Junt T, Wagers AJ, Mazo IB, von Andrian UH. Immunosurveillance by hematopoietic progenitor cells trafficking through blood, lymph, and peripheral tissues. Cell. 2007; 131:994–1008. [PubMed: 18045540]
47. Nagai Y, Garrett KP, Ohta S, Bahrun U, Kouro T, Akira S, Takatsu K, Kincade PW. Toll-like receptors on hematopoietic progenitor cells stimulate innate immune system replenishment. Immunity. 2006; 24:801–812. [PubMed: 16782035]
48. Strober W, Fuss IJ, Blumberg RS. The immunology of mucosal models of inflammation. Annu. Rev. Immunol. 2002; 20:495–549. [PubMed: 11861611]
49. Fuss IJ, Heller F, Boirivant M, Leon F, Yoshida M, Fichtner-Feigl S, Yang Z, Exley M, Kitani A, Blumberg RS, et al. Nonclassical CD1d-restricted NK T cells that produce IL-13 characterize an atypical Th2 response in ulcerative colitis. J. Clin. Invest. 2004; 113:1490–1497. [PubMed: 15146247]
50. Heller F, Fuss IJ, Nieuwenhuis EE, Blumberg RS, Strober W. Oxazolone colitis, a Th2 colitis model resembling ulcerative colitis, is mediated by IL-13-producing NK-T cells. Immunity. 2002; 17:629–638. [PubMed: 12433369]
51. Aranda R, Sydora BC, McAllister PL, Binder SW, Yang HY, Targan SR, Kronenberg M. Analysis of intestinal lymphocytes in mouse colitis mediated by transfer of CD4+, CD45RB high T cells to SCID recipients. J. Immunol. 1997; 158:3464–3473. [PubMed: 9120308]
52. Macpherson AJ, Slack E, Geuking MB, McCoy KD. The mucosal firewalls against commensal intestinal microbes. Semin. Immunopathol. 2009; 31:145–149. [PubMed: 19707762]
53. Saunders A, Lamb T, Pascall J, Hutchings A, Dion C, Carter C, Hepburn L, Langhorne J, Butcher GW. Expression of GIMAP1, a GTPase of the immunity-associated protein family, is not up-regulated in malaria. Malar. J. 2009; 8:53. [PubMed: 19338674]
54. Kupfer R, Lang J, Williams-Skipp C, Nelson M, Bellgrau D, Scheinman RI. Loss of a gimap/ian gene leads to activation of NF-kappaB through a MAPK-dependent pathway. Mol. Immunol. 2007; 44:479–487. [PubMed: 16584774]
55. Casola S. Control of peripheral B-cell development. Curr. Opin. Immunol. 2007; 19:143–149. [PubMed: 17303401]
56. Tan JT, Dudl E, LeRoy E, Murray R, Sprent J, Weinberg KI, Surh CD. IL-7 is critical for homeostatic proliferation and survival of naive T cells. Proc. Natl. Acad. Sci. U.S.A. 2001; 98:8732–8737. [PubMed: 11447288]
57. Pellegrini M, Bouillet P, Robati M, Belz GT, Davey GM, Strasser A. Loss of Bim increases T cell production and function in interleukin 7 receptor-deficient mice. J. Exp. Med. 2004; 200:1189–1195. [PubMed: 15504823]
58. Gauld SB, Benschop RJ, Merrell KT, Cambier JC. Maintenance of B cell anergy requires constant antigen receptor occupancy and signaling. Nat. Immunol. 2005; 6:1160–1167. [PubMed: 16200069]

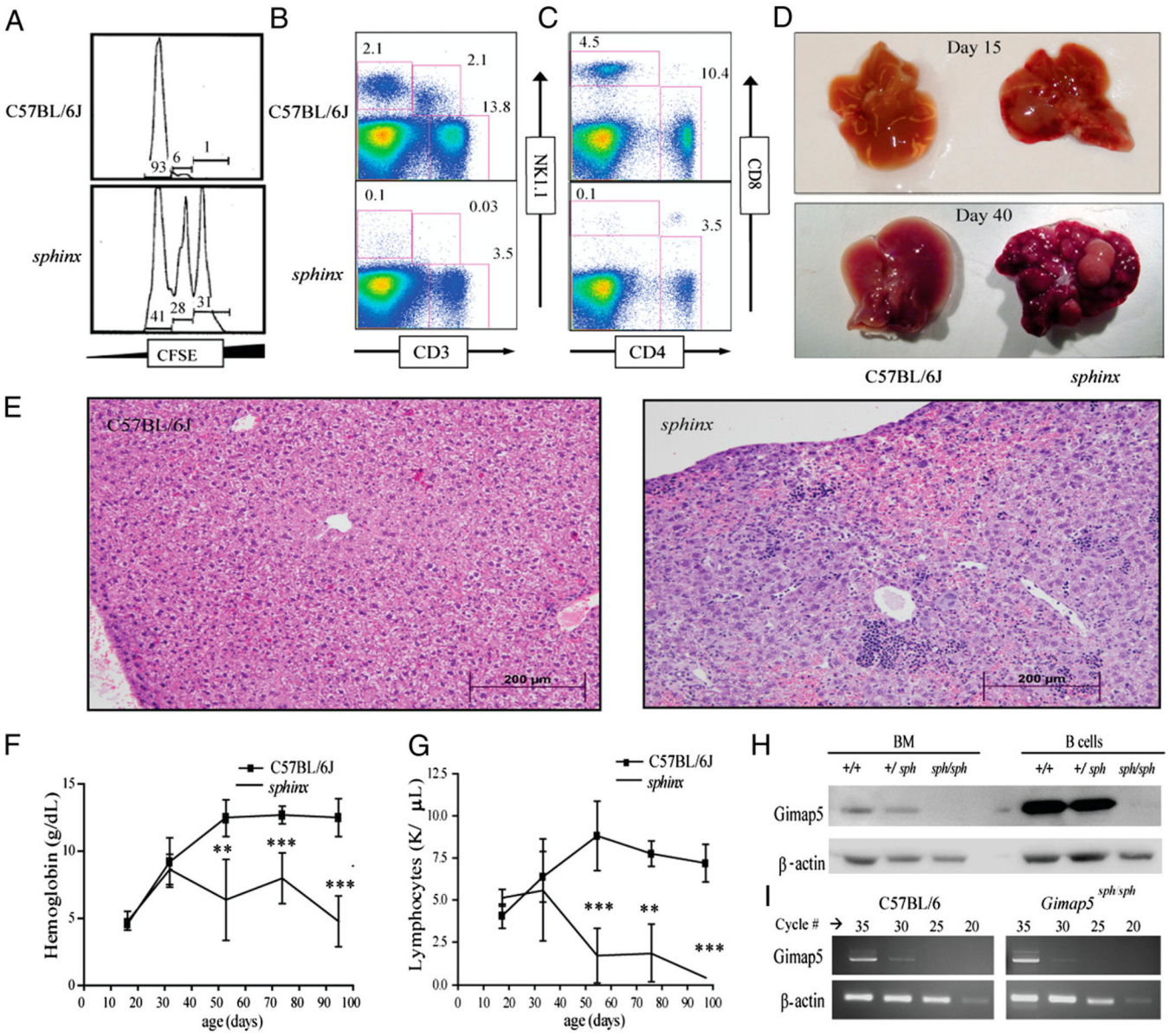

FIGURE 1.

Identification of *sphinx*, an ENU germline mutant exhibiting severe lymphopenia and hepatic extramedullary hematopoiesis. *A*, $CD8^+$ T cell and NK cell cytotoxicity were tested in ENU mutagenized mice that had been previously immunized with irradiated act-mOVA cells. Cytotoxic function was assessed by the ability to remove $\beta 2m^{-/-}$ ($CFSE^{int}$) NK cell or SIINFEKL-loaded ($CFSE^{high}$) $CD8^+$ T cell target cells. C57BL/6J control cells ($CFSE^{low}$) were used as a reference population. The percentage of $CD3^+$ T cells and $NK1.1^+$ NK cells (*B*), and $CD4^+$ and $CD8^+$ T cells (*C*) were quantified among splenocytes from 6-wk-old mice. *D*, Gross liver morphology in 15-d-old (*upper*) and 40-d-old (*lower*) mice. *E*, H&E staining of liver sections from 40-d-old mice (original magnification ×100). Circulating concentrations of hemoglobin (*F*) and lymphocytes (*G*) were measured in the blood of mice of various ages. SD is shown and statistical analyses were performed for each time point. *n*

= 5; **p < 0.01; ***p < 0.001. *H*, Gimap5 protein expression was measured in lysates of total bone marrow and purified splenic $CD19^+$ B cells. *I, Gimap5* RNA levels in purified splenic $CD19^+$ B cells isolated from C57BL/6J and $Gimap5^{sph/sph}$ mice were measured by RT-PCR. All analyses were performed at least three times.

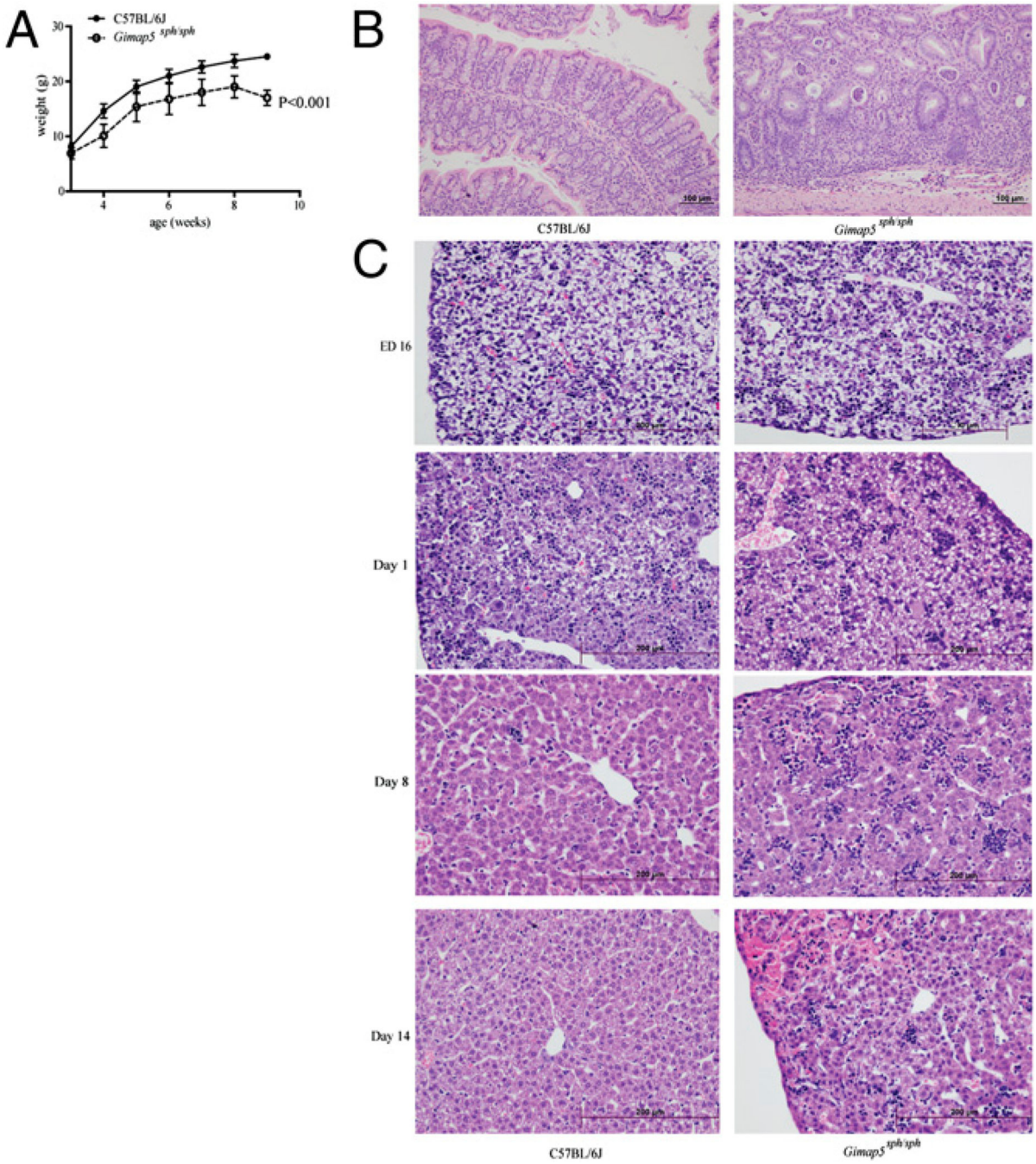

FIGURE 2.

Gimap5$^{sph/sph}$ mice develop wasting disease, colitis and aberrant hematopoiesis. *A*, Cohoused C57BL/6J and *Gimap5*$^{sph/sph}$ males were weighed at indicated ages. SEMis shown for each time point (n = 6) and statistical analysis was performed using a two-tailed paired t test. *B*, H&E-stained sections from the colon of 10-wk-old cohoused mice were assessed for intestinal inflammation (original magnification ×100). *C*, Hematopoietic cell egress from the neonatal liver was monitored by examining H&E-stained sections from

livers obtained at indicated developmental time-points (original magnification ×200). At least three livers were analyzed for each time point, and representative sections are shown.

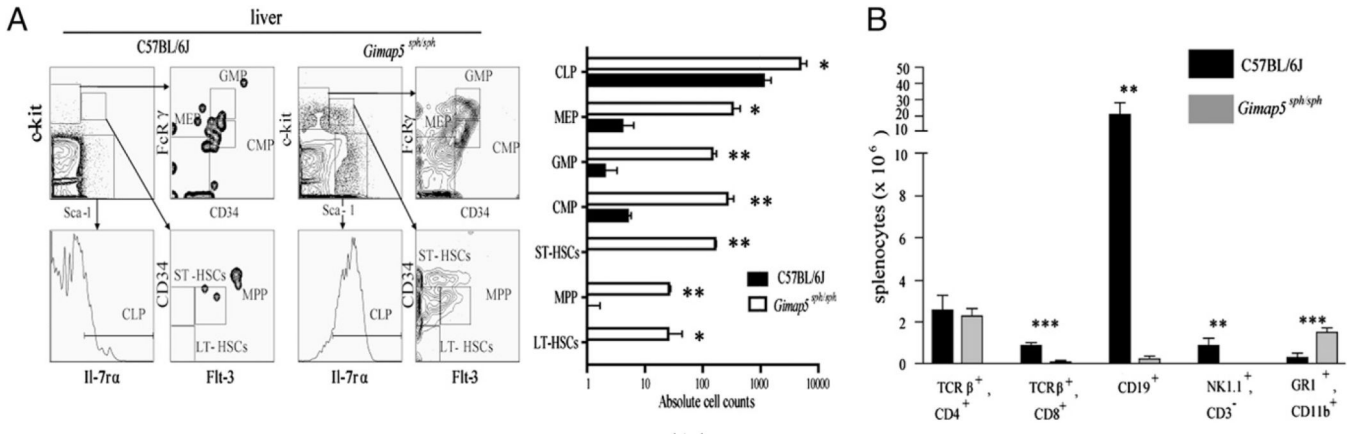

FIGURE 3.

Hematopoietic defects in the adult and fetal liver of *Gimap5*$^{sph/sph}$ mice. *A*, HSCs and hematopoietic precursor cells in the liver of 6-wk-old mice were analyzed by flow cytometry. The mean number of cells for each subset is indicated along with SEM. $n = 3$; *$p < 0.05$; **$p < 0.01$. *B*, Irradiated (1000 rad γ-radiation) *Rag2*$^{-/-}$ *Il2rγ*$^{-/-}$ recipient mice were reconstituted with ED 19 fetal liver cells. Six weeks later, splenocyte populations in chimeric mice were quantified by flow cytometry. The mean total number of each cell type in the spleen is shown along with SD. $n = 3$; **$p < 0.01$; ***$p < 0.001$.

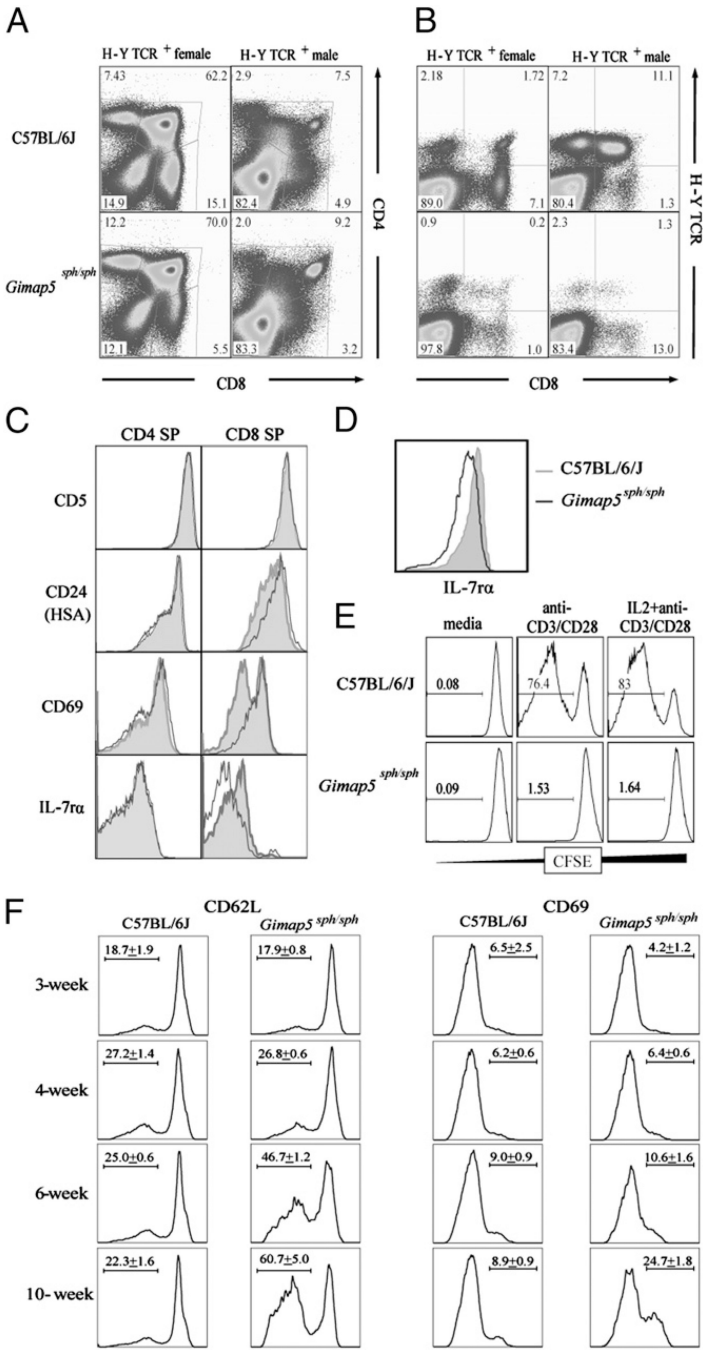

FIGURE 4.

T cell development and function in *Gimap5*$^{sph/sph}$ mice. To assess positive and negative selection, thymocyte (*A*) and splenocyte (*B*) populations from H-Y TCR^{+} transgenic mice of both genders were quantified and the average percentage of cells in each quadrant is shown. *C*, Expression of terminal thymocyte maturation markers—CD5, CD24, CD69, and IL-7Rα—was compared between C57BL/6J (shaded, gray) and *Gimap5*$^{sph/sph}$ (open, dark line) TCRβ^{+} CD4 SP and CD8 SP thymocytes. *D*, Surface expression of IL-7rα was measured in splenic CD4^{+} T cells. *E*, Proliferation of CFSE-labeled CD4^{+} T cells isolated from 8-wk-old

mice was assessed 96 h after stimulation with anti-CD3/CD28, with or without exogenous IL-2. *F*, Expression of CD62L and CD69 was measured on splenic $CD4^+$ T cells from 3-, 4-, 6- and 10-wk-old mice. Numbers represent mean ± SD. All analyses were performed at least twice.

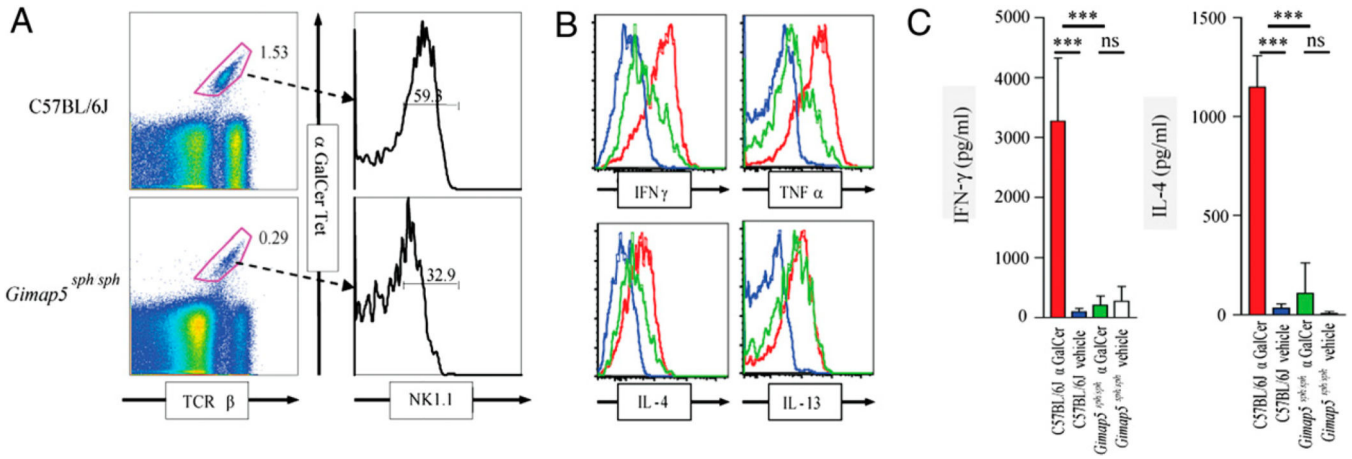

FIGURE 5.

Reduced *i*NKT cell survival and aberrant αGal-Cer-induced cytokine responses in *Gimap5*$^{sph/sph}$ mice. *A*, *i*NKT cells in the spleen of 6-wk-old *Gimap5*$^{sph/sph}$ mice were identified by αGal-Cer-loaded CD1d–tetramer binding and quantified by flow cytometry. *B*, Cytokine production was measured 90 min after injection of the *i*NKT cell agonist αGal-Cer on a per cell basis by intracellular staining for IFN-γ, TNF-α, IL-4, or IL-13 expression among αGal-Cer-loaded CD1d-tetramer^{+} *i*NKT cells (blue, unstimulated C57BL/6J; red, stimulated C57BL/6J; green, stimulated *Gimap5*$^{sph/sph}$). *C*, Serum cytokine concentrations of IFN-γ and IL-4 were also measured by ELISA 90 min after injection of αGal-Cer. SD is shown. $n = 3$; ***$p < 0.001$.

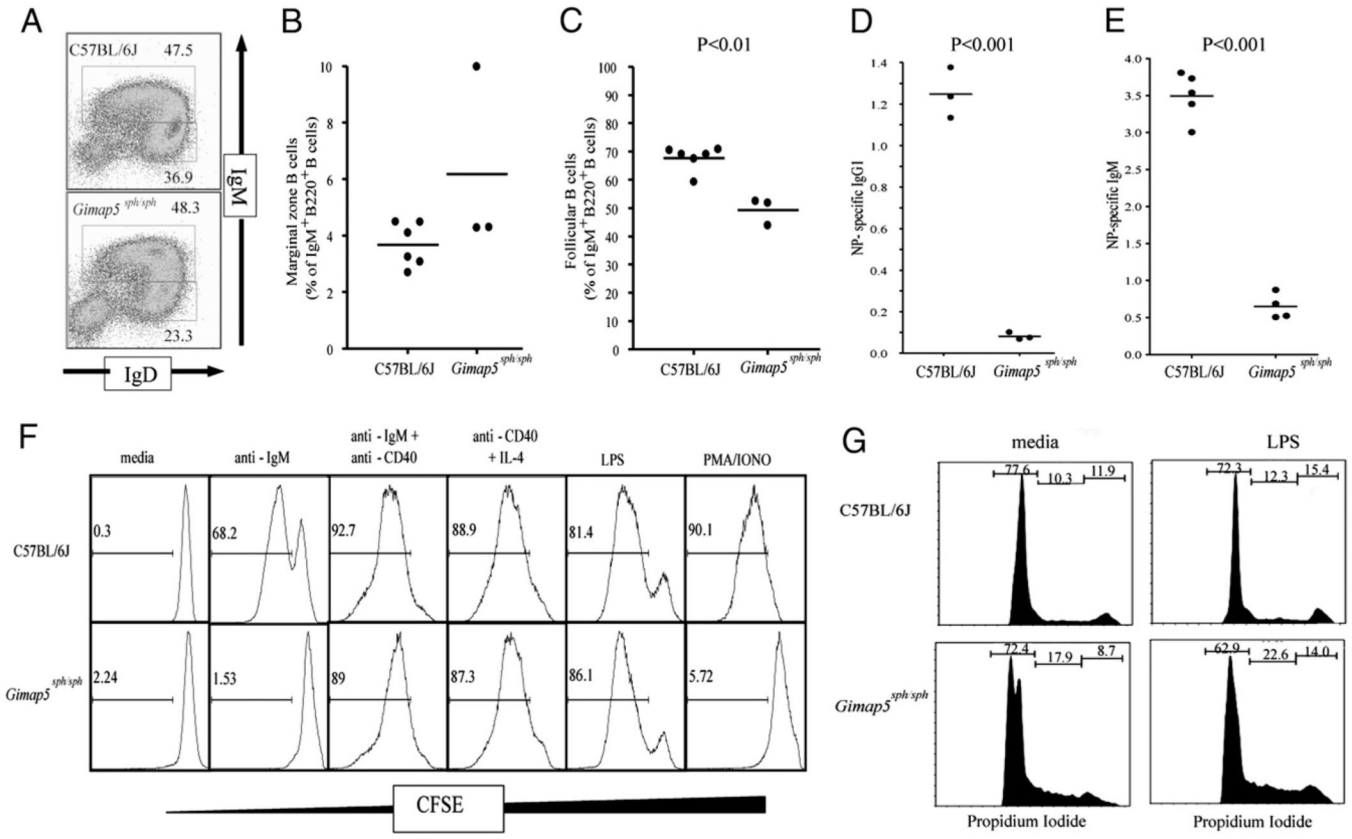

FIGURE 6.

Impaired BCR-dependent proliferation in *Gimap5*$^{sph/sph}$ B cells. *A–C*, Among CD19^{+} splenocytes from 6-wk-old mice, the percentage of IgM^{high} IgD^{int} naive and IgM^{low} IgD^{high} mature B cells (*A*) and the percentage of CD21^{high} CD23^{low} marginal zone (*B*) and CD21^{high} CD23^{high} follicular B cells (*C*) were determined. Six-week-old mice were immunized with 50 μg NP36-CGG with alum and LPS or 50 μg of NP50-Ficoll to assess T-dependent (*D*) or T-independent (*E*) Ab responses. NP-specific serum Abs were measured 14 d after immunization by ELISA. *F*, To assess B cell proliferation, CFSE-labeled CD19^{+} splenocytes were cultured in vitro for 90 h with media alone or with anti-IgM-Fab (10 μg/ml), LPS (2 μg/ml), anti-CD40 (10 μg/ml) plus IL-4 (10 ng/ml), or PMA (50 ng/ml) and ionomycin (500 ng/ml). *G*, Cell cycle progression of B cells cultured in the presence or absence of LPS was measured by propidium iodide staining after 48 h of incubation.

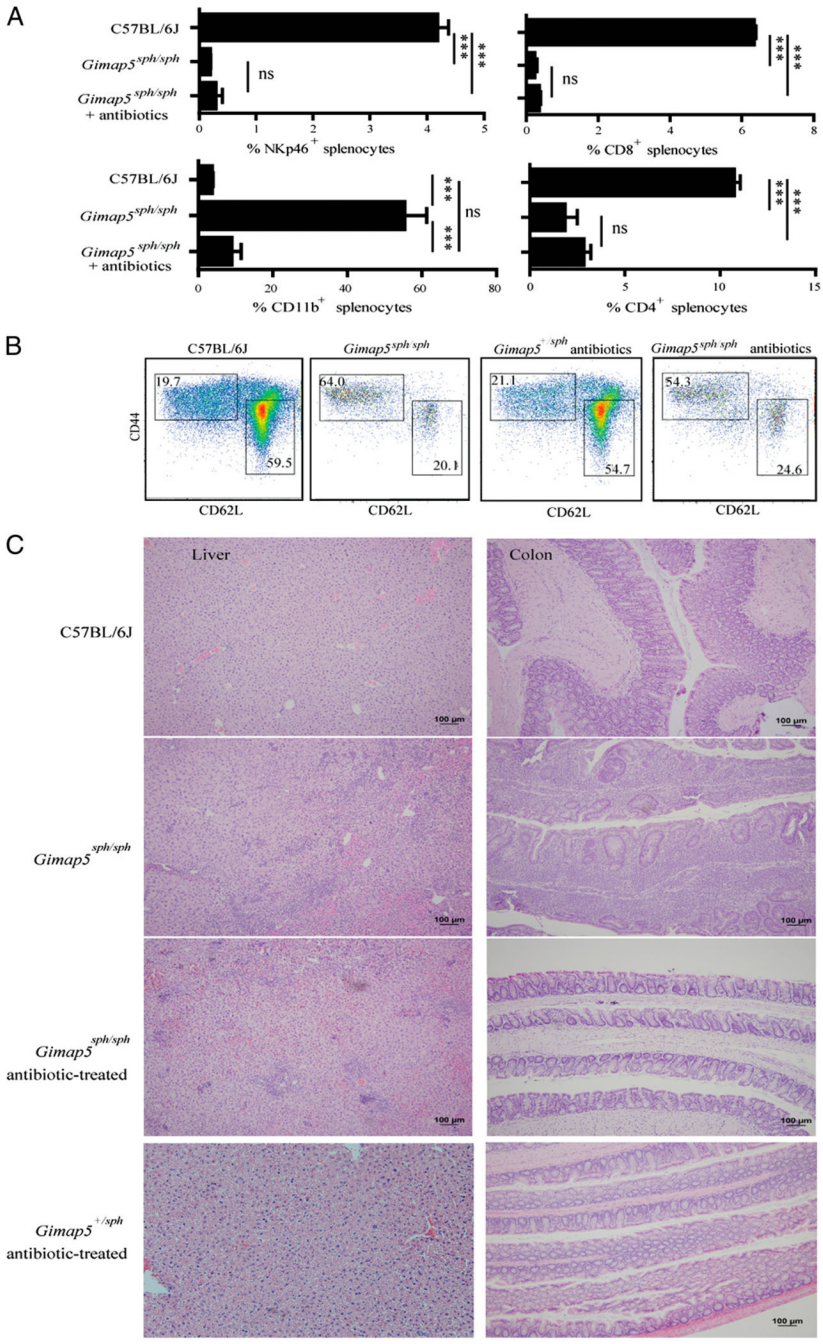

FIGURE 7.

Antibiotic treatment abrogates colitis but not lymphopenia and hepatic extramedullary hematopoiesis in *Gimap5*$^{sph/sph}$ mice. The percentage of NKp46^{+}, CD8^{+}, CD4^{+}, and CD11b^{+} splenocytes (*A*) and splenic CD44^{high} CD62L^{low} CD4^{+} T cells (*B*) in 9-wk-old C57BL/6J, *Gimap5*$^{sph/sph}$, and antibiotic-treated *Gimap5*$^{sph/sph}$ mice was determined. Bars represent mean values ± SEM. $n = 3$ per group; ***$p < 0.001$. *C*, H&E-stained sections from the colons and livers of 9-wk-old cohoused mice were assessed for extramedullary

hematopoiesis and intestinal inflammation (original magnification ×100). Representative histology from each group is shown. $n = 3$.

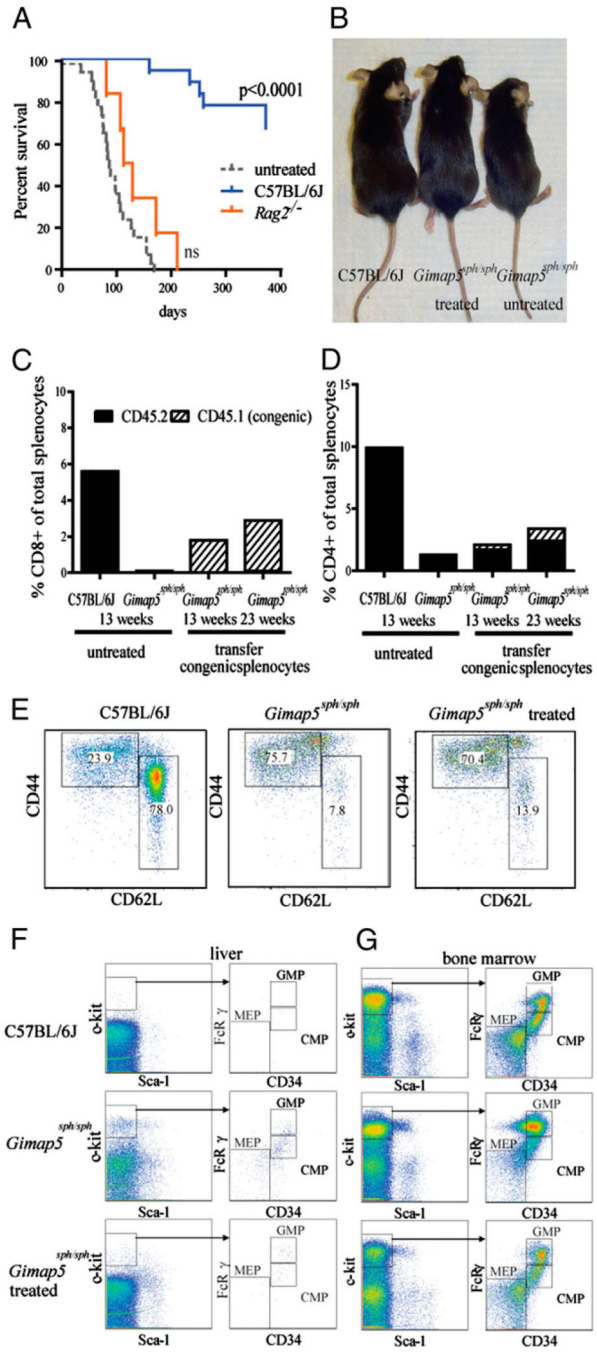

FIGURE 8.

Prevention of wasting disease by adoptive transfer of splenocytes. *A*, Twenty-five- to-35-d-old *Gimap5*$^{sph/sph}$ mice were injected with 1 × 10^{7} splenocytes from C57BL/6J or *Rag2*$^{-/-}$ donors. The survival of recipient mice was monitored for up to 9 mo (n ≥ 6 per group) and differences were statistically analyzed using the Gehan-Breslow-Wilcoxon test. *B*, *Gimap5*$^{sph/sph}$ mice injected with C57BL/6J splenocytes did not develop wasting disease. Representative 15-wk-old mice are shown. *C* and *D*, In 30-d-old *Gimap5*$^{sph/sph}$ mice injected with congenically marked splenocytes, the percentages of transferred (CD45.1) and

endogenous (CD45.2) $CD8^+$ T cells (*C*) and $CD4^+$ T cells (*D*) were determined at the indicated time points after transfer. *E*, Expression of CD62L and CD44 on splenic $CD4^+$ T cells from 13-wk-old C57BL/6 mice, *Gimap5*$^{sph/sph}$ mice, and *Gimap5*$^{sph/sph}$ mice injected with $CD45.1^+$ congenic splenocytes (only cells of *Gimap5*$^{sph/sph}$ origin are shown). Lin myeloid precursor cells were quantified in the liver (*F*) and bone marrow (*G*) of 15-wk-old mice.